JACC: BASIC TO TRANSLATIONAL SCIENCE VOL. 5, NO. 6, 2020

PRECLINICAL RESEARCH

Impact of Coronary Atherosclerosis on Bioresorbable Vascular Scaffold Resorption and Vessel Wall Integration

Yanping Cheng, MD,[a] Marco Ferrone, MD,[a] Qing Wang, MD, PhD,[b] Laura E.L. Perkins, DVM, PhD,[b] Jennifer McGregor, BS,[a] Björn Redfors, MD, PhD,[a] Zhipeng Zhou, MA,[a] Richard Rapoza, PhD,[b] Gerard B. Conditt, RCIS,[a] Aloke Finn, MD,[c] Renu Virmani, MD,[c] Grzegorz L. Kaluza, MD, PhD,[a] Juan F. Granada, MD[a]

VISUAL ABSTRACT

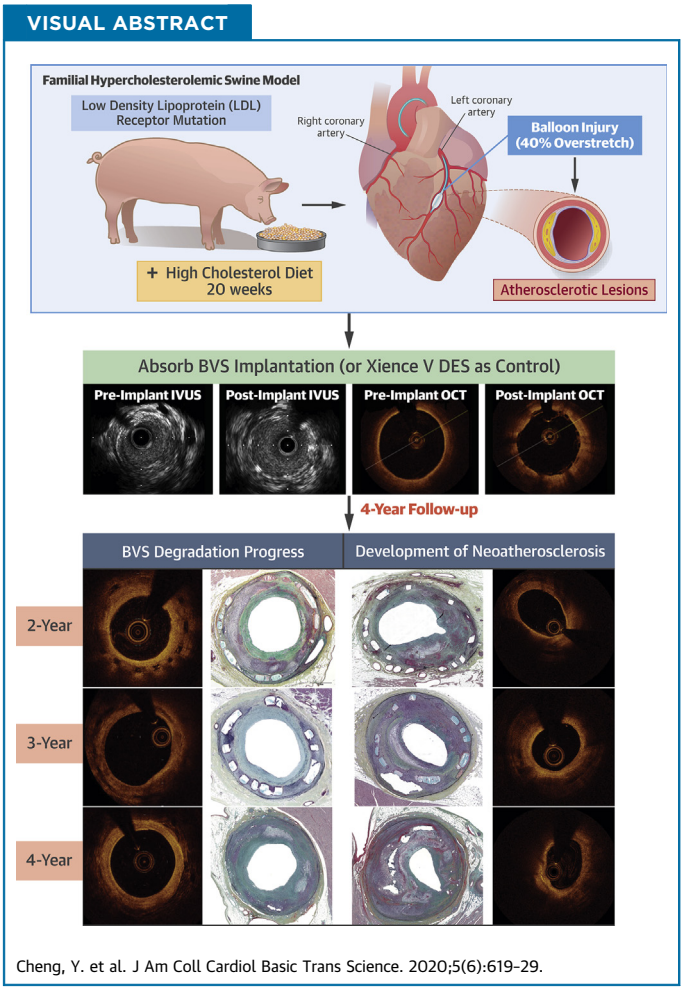

Cheng, Y. et al. J Am Coll Cardiol Basic Trans Science. 2020;5(6):619-29.

From the [a]CRF Skirball Center for Innovation, Orangeburg, New York; [b]Abbott Vascular, Santa Clara, California; and the [c]CVPath Institute, Inc., Gaithersburg, Maryland. This study was sponsored by Abbott Vascular, Santa Clara, California. Dr. Wang is an employee of Abbott Laboratories. Dr. Perkins is an employee of and shareholder in Abbott Laboratories. Dr. Rapoza is an employee

ISSN 2452-302X https://doi.org/10.1016/j.jacbts.2020.04.005

ABBREVIATIONS AND ACRONYMS

BVS = bioresorbable vascular scaffold

EES = everolimus-eluting stent

FHS = familial hypercholesterolemic swine

IVUS = intravascular ultrasonography

OCT = optical coherence tomography

HIGHLIGHTS

- **The bioresorption process of the Absorb BVS has been directly characterized only in a normal swine model and indirectly (by imaging surrogates) in clinical studies.**
- **Using multimodality imaging and histology, this study indicates that in a diseased animal model, the resorption and integration of BVS into the arterial wall is not affected by the presence of untreated hyperlipidemia and atherosclerosis progression.**
- **Imaging and histology suggest that BVS degradation progresses similarly in the presence of atherosclerosis compared with earlier data from nonatherosclerotic arteries. However, BVS is not immune to the development of neoatherosclerosis.**

SUMMARY

The integration of the Absorb bioresorbable vascular scaffold (BVS) into the arterial wall has never been tested in an in vivo model of atherosclerosis. This study aimed to compare the long-term (up to 4 years) vascular healing responses of BVS to an everolimus-eluting metallic stent in the familial hypercholesterolemic swine model of atherosclerosis. The multimodality imaging and histology approaches indicate that the resorption and vascular integration profile of BVS is not affected by the presence of atherosclerosis. BVS demonstrated comparable long-term vascular healing and anti-restenotic efficacy to everolimus-eluting metallic stent but resulted in lower late lumen loss at 4 years.

The clinical efficacy of metallic drug-eluting stents has been well established (1,2), although long-term clinical events related to in-stent restenosis and late stent thrombosis continue to accrue over time (3). The permanent caging of the treated artery by a metallic stent has been proposed to be an important contributor to late device failure (4). It has been hoped that bioresorbable scaffolds will overcome this limitation by allowing the return of vasomotion and elasticity in the treated segment and, eventually, also by late lumen gain and stabilization of the atherosclerotic process at the treated site. Randomized controlled trials comparing the Absorb bioresorbable vascular scaffold (BVS) with metallic everolimus-eluting stents (EES) showed similar clinical efficacy up to 1 year (5). However, meta-analysis of pooled individual patient data from the ABSORB trials at 2 and 3 years showed increased rates of adverse events for BVS compared with EES (6,7). The reasons for this unexpected adverse long-term result are not fully understood. Although experimental studies in healthy swine show that the Absorb BVS is completely resorbed by approximately 3 years (8), the integration of the BVS has never been tested with in vivo models of atherosclerosis. In this study, we aimed to evaluate the long-term (4 years) biological effect of BVS on vascular adaptation and strut resorption compared with EES in the familial hypercholesterolemic swine (FHS) model of spontaneous atherosclerosis using endovascular imaging techniques and histology.

METHODS

EXPERIMENTAL DESIGN. The study was approved by the Institutional Animal Care and Use Committee and conducted in accordance with the Animal Welfare Act and the Guide for the Care and Use of Laboratory Animals (National Research Council, National Institutes of Health publication no. 85-23, revised 1996) at U.S. Department of Agriculture-licensed, Association for the Assessment and Accreditation of

of Abbott Laboratories. All other authors have reported that they have no relationships relevant to the contents of this paper to disclose.
The authors attest they are in compliance with human studies committees and animal welfare regulations of the authors' institutions and Food and Drug Administration guidelines, including patient consent where appropriate. For more information, visit the *JACC: Basic to Translational Science* author instructions page.

Manuscript received December 20, 2019; revised manuscript received April 2, 2020, accepted April 6, 2020.

FIGURE 1 Study Design

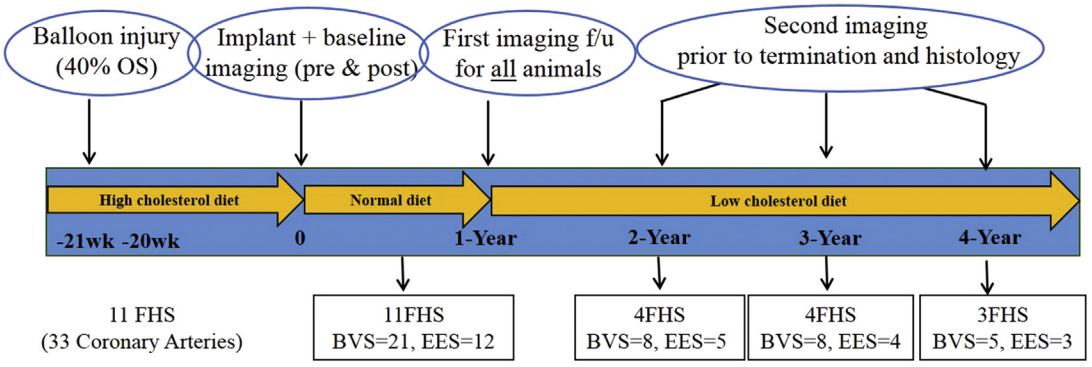

BVS = bioresorbable vascular scaffold; EES = everolimus-eluting stent; FHS = familial hypercholesterolemic swine; f/u = follow-up; OS = overstretch.

Laboratory Animal Care International-accredited animal research facility.

The study flowchart is shown in Figure 1. Interim imaging assessments, including coronary angiography, intravascular ultrasonography (IVUS), and optical coherence tomography (OCT) were performed at 1-year follow-up for all the animals (n = 11). At 2 (n = 4), 3 (n = 4), and 4 (n = 3) years, animals were killed for histology evaluation after imaging analysis.

THE FHS MODEL. Eleven FHS (10 ± 0.07 months of age; weight: 70.8 ± 7.1 kg) were used in this study. Mean cholesterol levels at baseline was 709 ± 90 mg/dl (range 612 to 956 mg/dl). The genotypic and clinical characteristics and response to stent implantation of this model have been published (9). Animals were maintained on a low-grade high-cholesterol diet (0.6% cholesterol) for the first 21 weeks to accelerate lesion development. At device implantation, the mean cholesterol level was 654 ± 65 mg/dl, and the animals were switched to a standard porcine diet, yet cholesterol level remained markedly elevated at the end of the study at 361 ± 64 mg/dl.

CORONARY INJURY AND DEVICE IMPLANTATION PROCEDURE. Under general anesthesia, arterial access was obtained, and activated clotting time of ≥250 s was achieved. Proximal coronary segments were balloon-injured, targeting at least approximately 40% overstretch (day 0) (10). Twenty weeks after initial injury, either BVS (n = 21; 3.0 × 18 mm or 3.5 × 18 mm) or EES (n = 12; 3.5 × 18 mm or 4.0 × 18 mm) were implanted in the previously injured segments, targeting a device-to-artery ratio of 1.1:1, under angiographic guidance. All animals received oral aspirin (81 mg) and clopidogrel (75 mg) once daily beginning 1 day before injury and implantation procedures and continued for 30 days post-injury and throughout the first year post-implantation.

QUANTITATIVE CORONARY ANGIOGRAPHY ANALYSIS. Quantitative coronary angiography analysis was performed with QAngio XA Software, version 7.1.14.0 (Medis Medical Imaging System, Leiden, the

TABLE 1 Quantitative Coronary Angiography Analysis

Time Point/Parameter	BVS	EES	p Value
Baseline	21	12	
% Pre-implantation DS	12.05 ± 8.89	9.05 ± 7.06	0.325
Device-to-artery ratio	1.18 ± 0.12	1.26 ± 0.08	0.036
Post-implantation MLD, mm	2.79 ± 0.44	3.70 ± 0.28	<0.001
1-yr follow-up	21	12	
RVD, mm	3.30 ± 0.64	3.95 ± 0.51	0.005
MLD, mm	2.22 ± 0.32	3.04 ± 0.61	0.006
%DS	36.9 ± 9.6	31.2 ± 17.6	0.319
Late lumen loss, mm	1.02 ± 0.32	1.15 ± 0.67	0.517
2-yr follow-up	8	5	
RVD, mm	3.09 ± 0.31	3.63 ± 0.38	0.017
MLD, mm	1.98 ± 0.34	2.65 ± 0.42	0.010
%DS	24.4 ± 11.9	26.9 ± 9.8	0.701
Late lumen loss, mm	0.69 ± 0.41	0.98 ± 0.38	0.240
3-yr follow-up	8	4	
RVD, mm	2.77 ± 0.36	3.30 ± 0.61	0.085
MLD, mm	1.80 ± 0.46	2.27 ± 0.93	0.253
%DS	36.9 ± 13.7	37.5 ± 25.0	0.956
Late lumen loss, mm	1.03 ± 0.35	1.35 ± 0.86	0.527
4-yr follow-up	5	3	
RVD, mm	3.55 ± 0.82	3.85 ± 0.70	0.612
MLD, mm	1.85 ± 0.64	1.83 ± 0.22	0.954
%DS	39.2 ± 16.0	53.4 ± 2.6	0.118
Late lumen loss, mm	1.14 ± 0.37	2.09 ± 0.12	0.006

Values are n or mean ± SD.

DS = diameter stenosis; MLD = minimal lumen diameter; RVD = reference vessel diameter; other abbreviations as in Figure 1.

TABLE 2 IVUS Parameter Changes Between 1 and 2, 1 and 3, and 1 and 4 Years

	BVS	EES	p Value
1- to 2-yr follow-up interval	8	5	
Lumen area			
Absolute change, mm^2	0.83 ± 1.11	-0.34 ± 1.93	0.186
% change	19 ± 21	-2 ± 20	0.105
Vessel area			
Absolute change, mm^2	0.64 ± 1.78	-0.28 ± 3.10	0.509
% change	6 ± 17	-2 ± 15	0.423
Total plaque area			
Absolute change, mm^2	-0.19 ± 1.34	0.06 ± 4.09	0.897
% change	-1 ± 27	-1 ± 38	0.973
1- to 3-yr follow-up interval	8	4	
Lumen area			
Absolute change, mm^2	1.42 ± 2.07	0.45 ± 2.14	0.466
% change	31 ± 54	1 ± 33	0.333
Vessel area			
Absolute change, mm^2	5.47 ± 6.02	2.20 ± 2.35	0.328
% change	54 ± 56	15 ± 17	0.100
Total plaque area			
Absolute change, mm^2	4.03 ± 6.65	1.75 ± 3.45	0.541
% change	61 ± 94	24 ± 51	0.484
1- to 4-yr follow-up interval	5	3	
Lumen area			
Absolute change, mm^2	0.21 ± 0.95	-2.37 ± 1.25	0.026
% change	3 ± 15	-25 ± 9	0.039
Vessel area			
Absolute change, mm^2	3.60 ± 5.88	3.58 ± 1.82	0.996
% change	26 ± 42	20 ± 10	0.810
Total plaque area			
Absolute change, mm^2	2.82 ± 5.68	5.95 ± 2.32	0.408
% change	34 ± 76	70 ± 31	0.470

Values are n or mean ± SD.
IVUS = intravascular ultrasonography; other abbreviations as in Figure 1.

Netherlands). A contrast-filled catheter was used for calibration; the minimum lumen diameter (MLD) was obtained from a single view with the lowest measurement, and the reference vessel diameter was automatically calculated. Percent diameter stenosis (%DS) was calculated from the MLD and the reference vessel diameter.

GRAY-SCALE IVUS ANALYSIS. IVUS pullback images were generated (Atlantis SR Pro 40MHz catheters and iLab system; Boston Scientific, Natick, Massachusetts) and analyzed with commercially available software (echoPlaque, Indec Systems Inc., Santa Clara, California). Luminal, device, and vessel areas were measured, and the neointimal and total plaque areas were calculated. To normalize the lumen changes to the variations in the reference vessel size, patency ratio was calculated as: (follow-up lumen area in the implanted segment)/(follow-up reference vessel lumen area), and its changes were also evaluated at different time points (11).

OCT IMAGE ACQUISITION AND ANALYSIS. OCT images were obtained with the C7-XR OCT imaging system (LightLab Imaging, Inc., St. Jude Medical, St. Paul, Minnesota). Qualitative analyses were performed at 1-mm intervals with commercial software (ILUMIEN OPTIS; St. Jude Medical). Cross-section lumen, device areas, and percent area stenosis were measured. Alterations of the BVS struts in their optical appearance at follow-up were categorized into 4 subgroups that have been applied in the preclinical study (12): preserved box, open box, dissolved bright box, and dissolved black box.

HISTOLOGICAL ANALYSIS. An independent pathology laboratory (CVPath Institute Inc., Gaithersburg, Maryland) conducted the histological analysis. Sections were collected and stained with hematoxylin and eosin and Movat's pentachrome as previously described (8). Vessel injury (range 0 to 3), neointimal inflammation (range 0 to 4), adventitial inflammation (range 0 to 3), and fibrin (range 0 to 3) were semi-quantitatively scored for each section as previously described (8). All sections were also evaluated for the presence of neoatherosclerosis, which is defined as the presence of foam cells, cholesterol clefts, and/or calcification in the neointima (13), and assigned a score from 0 to 3 (14).

STATISTICAL ANALYSIS. Statistical analysis was conducted with SAS, version 9.4 (SAS Institute, Cary, North Carolina). Values are expressed as the mean ± SD. Groups (BVS and EES) were compared at each time point using Student's *t*-test. Select IVUS and OCT parameters were also compared between animal cohorts killed at 1 year and subsequent time points (1 to 2, 1 to 3, and 1 to 4 years), also by means of Student's *t*-test. $p < 0.05$ was considered significant.

RESULTS

QUANTITATIVE CORONARY ANGIOGRAPHY ANALYSIS. No complications occurred at the time of balloon injury and device implantation. Table 1 summarizes the quantitative coronary angiography analysis data. The degree of balloon injury achieved in the 2 groups was comparable (balloon-to-artery ratios: BVS, 1.55 ± 0.15 vs. EES, 1.43 ± 0.16; $p = 0.051$). At the time of device implantation, the mean pre-implantation %DS and implant-to-artery ratios were also comparable between BVS and EES. Post-implantation MLD was larger with EES than BVS due to the fact that larger (>3.5 mm) BVS were not available at the time of the study (Table 1). Angiographic late lumen loss and %DS were not significantly different between BVS and EES at 1, 2, and 3-year follow-up time points. At 4 years, despite the difference in device size used in this study favoring

FIGURE 2 Key Quantitative IVUS Data From Day 0 to 4 Years of Follow-Up

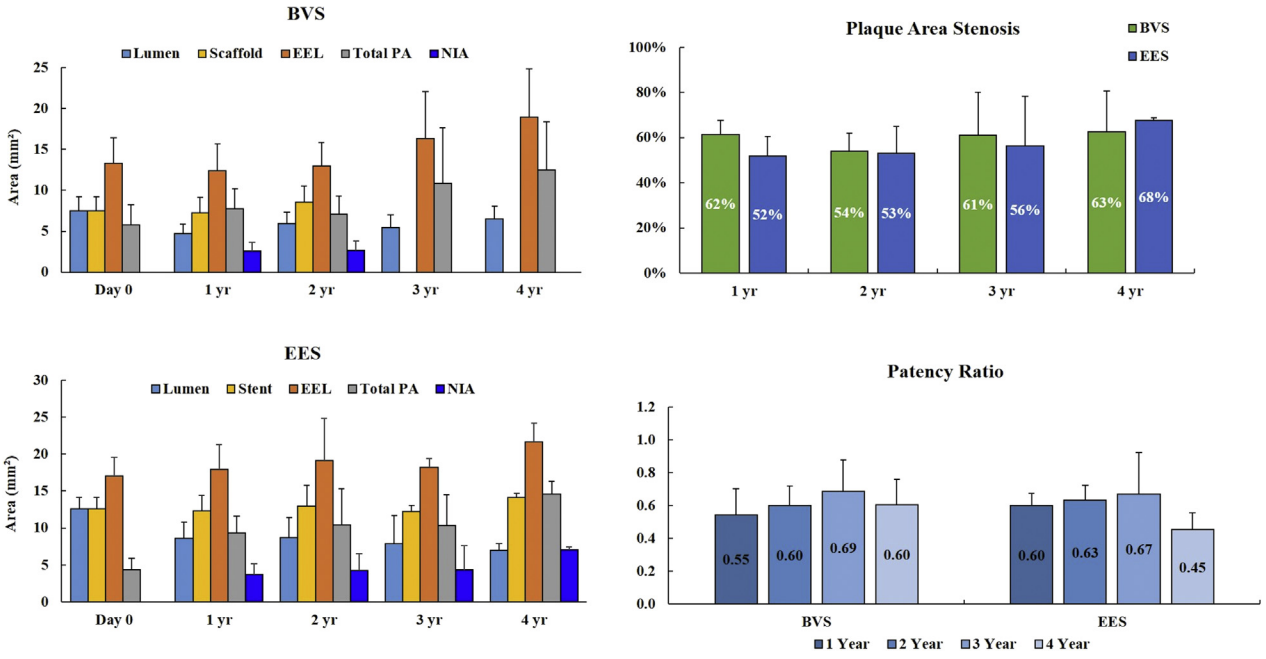

Lumen, scaffold/stent, vessel (EEL), neointimal, and total plaque area (PA) changes by IVUS from baseline (post-implantation) to 4 years. The vessel area and total plaque area were increased in both groups at 3 and 4 years. There was no difference in the percent PA stenosis between the 2 devices at all time points. The patency ratio of BVS-treated vessels remained unchanged from 2 to 4 years but decreased in the EES-treated vessels at 4 years. NIA = neointimal area; other abbreviations as in Figure 1.

EES, BVS showed lower late lumen loss than EES (BVS: 1.14 ± 0.37 vs. EES: 2.09 ± 0.12; p = 0.0056), whereas the difference in %DS between the 2 devices was not significant at this time point (Table 1).

GRAY-SCALE IVUS. Twenty weeks after injury, a comparable degree of plaque burden (% area stenosis) before device implantation was found in both groups (BVS: 25.5 ± 10.3% vs. EES: 22.1 ± 4.6%; p = 0.207). An overall summary of IVUS data from post-implantation to 4 years is presented in Table 2 and Figure 2. The implanted scaffolds were no longer discernible by IVUS by 3 years; thus, only lumen and vessel areas were measured. The average vessel area for all devices of each type that were available for analysis at each time point appeared to be higher at later time points than at baseline (BVS: baseline [n = 21], 13.31 ± 3.12 mm^2 vs. 1 year [n = 21], 12.42 ± 3.27 mm^2 vs. 2 years [n = 8], 12.96 ± 2.92 mm^2 vs. 3 years [n = 8], 16.34 ± 5.73 mm^2 vs. 4 years [n = 4], 18.97 ± 5.89 mm^2; EES: baseline [n = 12], 16.99 ± 2.54 mm^2 vs. 1 year [n = 12], 17.95 ± 3.31 mm^2 vs. 2 years [n = 5], 19.14 ± 5.67 mm^2 vs. 3 years [n = 4], 18.23 ± 1.13 mm^2 vs 4 years [n = 3], 21.63 ± 2.53 mm^2; p = 0.281). Average total plaque areas were also higher in both groups at later time points than at baseline because of atherosclerosis progression (BVS: baseline, 5.82 ± 2.41 mm^2 vs. 1 year, 7.71 ± 2.50 mm^2 vs. 2 years, 7.05 ± 2.25 mm^2 vs. 3 years, 10.89 ± 6.80 mm^2 vs. 4 years, 12.47 ± 5.95 mm^2; EES: baseline, 4.39 ± 1.54 mm^2 vs. 1 year, 9.35 ± 2.27 mm^2 vs. 2 years 10.44 ± 4.87 mm^2 vs. 3 years 10.32 ± 4.14 mm^2 vs. 4 years 14.63 ± 1.70 mm^2). There was no difference in the percent plaque area stenosis between the 2 devices at any of the studied time points (Figure 2).

As summarized in Table 2, compared to 1-year values, the lumen area remained stable in BVS at 4 years but significantly decreased in EES. The patency ratio of BVS-treated vessels appeared stable between 2 and 4 years but dropped in the EES-treated vessels at 4 years (Figure 2).

OCT ANALYSIS. In all animals, the scaffold struts were no longer discernible along the length of the implanted segments by OCT at 4 years (Figure 3). The strut count and its optical appearance changed over time: the recognizable struts were decreased over time, with 95% of preserved box appearance at 1 year, 17% at 2 years, and 7% at 3 years; at 4 years, the struts were not discernible in any implanted segments (Figure 4). The overall OCT findings are summarized in Figure 5, top panels. In addition, relative OCT parameter differences from years 1 to 2, 1 to 3, and 1 to 4 for

FIGURE 3 Representative Angiographic and OCT Images

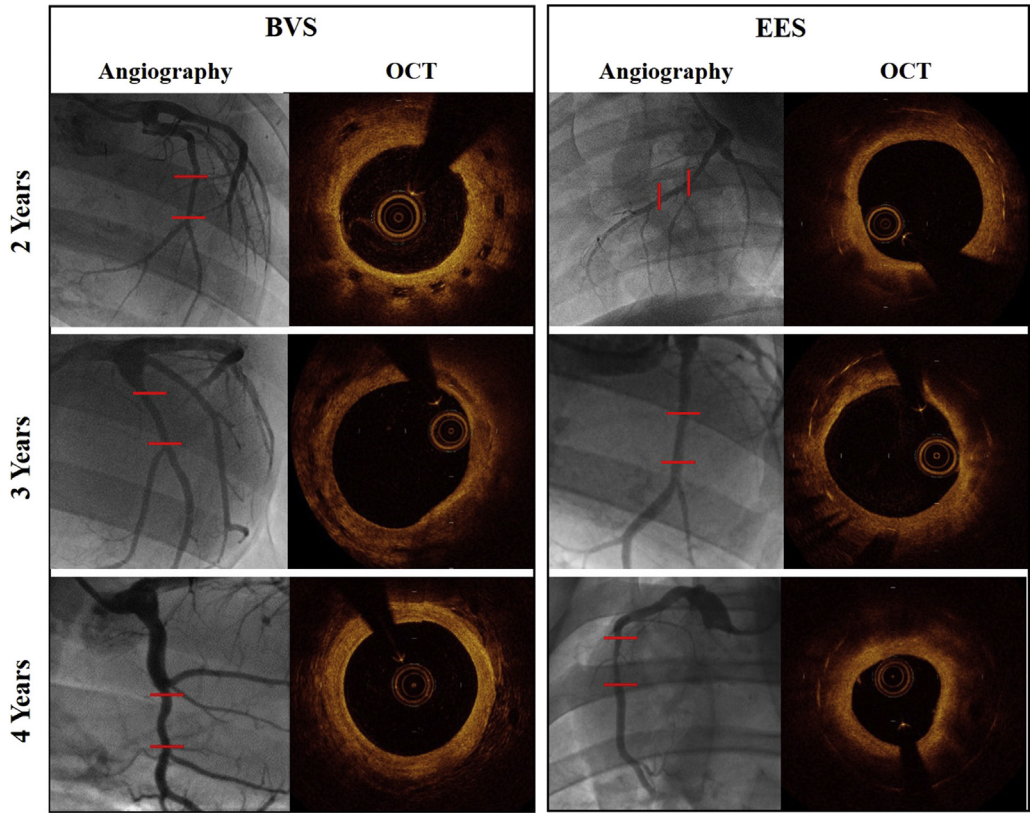

Representative angiography and OCT images of BVS and EES at 2, 3, and 4 years. The scaffold struts were no longer discernible by OCT at 4 years. OCT = optical coherence tomography; other abbreviations as in Figure 1.

both devices are summarized in Figure 5, bottom panels. Compared to 1 year, the scaffold area was higher by 15% at 2 years, and the mean lumen area was larger by 25% between 1 and 2 years and 37% between 1 and 3 years. Consistent with IVUS findings, the lumen area was significantly decreased by 34% in the EES group between 1 and 4 years, whereas no further lumen area changes were observed in the BVS group.

HISTOLOGICAL ANALYSIS. In all evaluated arteries, all lumens were widely patent, and struts were completely incorporated within neointimal growth (Figure 6). BVS struts at 2 years were readily visible as unstained rhombi sequestered within the neointima, whereas at 3 years, struts stained blue-green (Movat's pentachrome) and were faintly eosinophilic (hematoxylin and eosin) (Figures 6 and 7). Evidence of BVS dismantling, defined as stacking or misaligned struts, was observed infrequently at 2 and 3 years. At 4 years, BVS struts were difficult to discern and were mainly recognized as discrete foci of fibrous tissue, although blue-green-tinted irregular to rhomboid-shaped regions were rarely observed. In contrast to 2 years, birefringence under polarized light consistent with residual polymer was not observed at 4 years (Figure 6). For both BVS and EES, the neointimal growth was moderate to severe in thickness and composed of primarily proteoglycan with scattered smooth muscle cells from 2 to 4 years (Figure 6). Injury scores were moderate to marked; were comparable between BVS and EES at 2, 3, and 4 years; and were likely related to the advancement of atherosclerosis and inflammation for both implants. Neointimal inflammation was moderate to severe in both BVS and EES at 2, 3 and 4 years (Figure 8). Fibrin deposition and red blood cell extravasation were absent to minimal in both groups at each time point. Evidence of neoatherosclerosis was observed in both BVS and EES and included focal to focally extensive foam cells, calcification, cholesterol clefts, and necrotic cores starting at 2 years (Figure 7); the mean scores are provided in Figure 8. Similarly, the naive segments proximal and distal to both BVS and EES implants demonstrated

FIGURE 4 Changes in Optical Appearance of Struts Over Time ("Box Analysis")

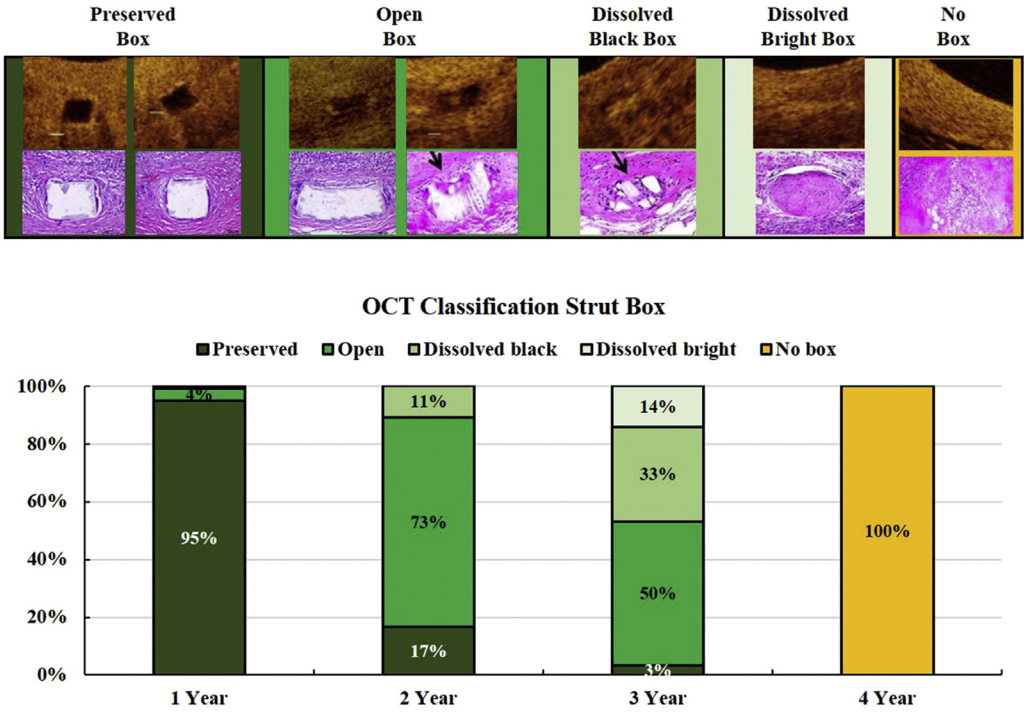

Alterations of the scaffold struts in their optical appearance were categorized into 4 subgroups: preserved box, open box, dissolved black box, and dissolved bright box. The recognizable struts were decreased over time, with 95% of preserved box appearance at 1 year, 17% at 2 years, and 7% at 3 years; at 4 years, the struts were not discernible in any implanted segments. OCT = optical coherence tomography.

marked atherosclerotic lesion progression at each time point, with foam cell accumulations, calcification, and cholesterol clefts (Figure 7).

DISCUSSION

In this study, we aimed to study the patterns of polymer resorption, vascular healing, and neoatherosclerosis development after BVS implantation in a swine model of spontaneous untreated atherosclerosis. At 4 years, the main findings of this study are as follows.

- The net effect on angiographic restenosis (lumen loss) was more favorable in BVS compared to EES.
- Imaging demonstrated that atherosclerotic plaque progression occurred in comparable proportions in relation to both devices; however, the expansive remodeling occurring in BVS resulted in a net lumen gain despite disease progression.
- The long-term healing profiles of both devices were comparable throughout all time points.
- Multi-modality imaging and histology confirmed that full strut resorption occurs between years 3 and 4; a timeline similar to that reported in normal healthy arteries.
- BVS are not immune to neoatherosclerosis development.

One of the most intriguing biological effects of BVS is the induction of expansive vascular remodeling with recovery of in-segment pulsatility observed from 12 to 48 months in healthy porcine coronary arteries (15). In the present study using atherosclerotic vessels, the scaffold and vessel area remained unchanged during the first year after scaffold implantation. Both IVUS and OCT confirmed evidence of expansive remodeling occurring after the second year. In contrast, progressive lumen loss continued in the EES group due to the permanent mechanical caging effect in the arterial wall. Overall, vessel and plaque/media area measured by IVUS increased over time in both devices. However, because of the expansive remodeling effect, the net effect of plaque progression on lumen loss over time is less pronounced in BVS compared to EES. Of note, a long-term study of BVS in normal swine has featured much less pronounced lumen loss and stenosis between 12 and 42 months post-implantation than

FIGURE 5 Lumen, Scaffold/Stent, and Neointimal Area Changes by OCT at 1 to 4 Years of Follow-Up

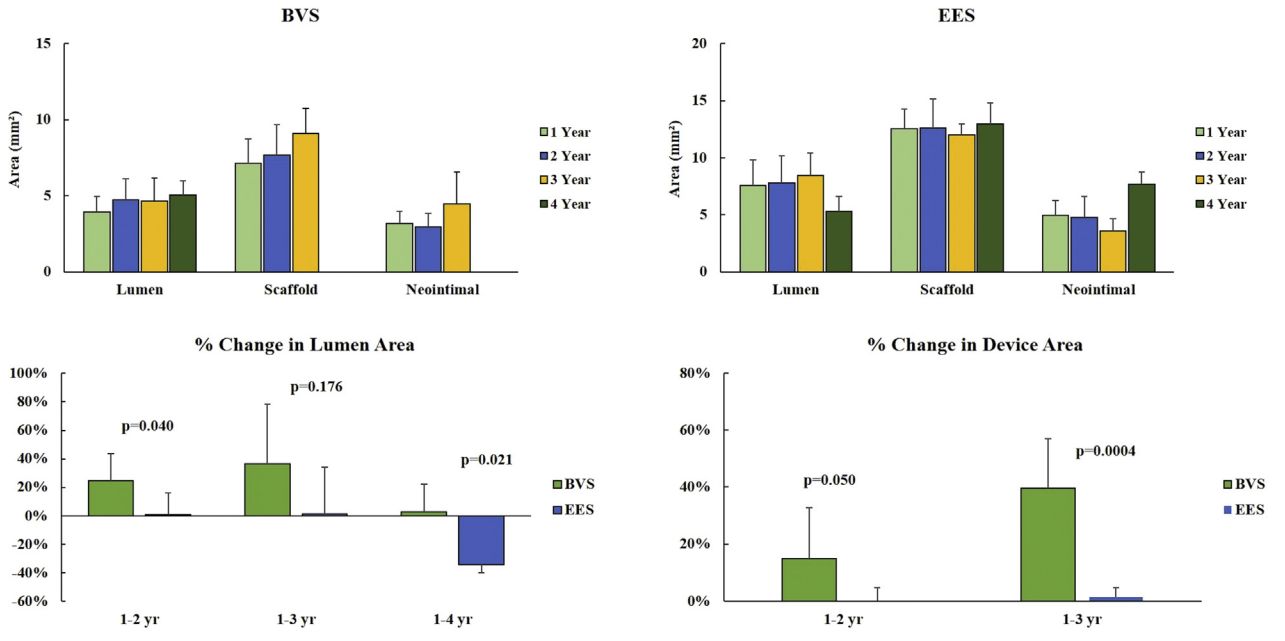

The scaffold and luminal area enlargements were observed in the BVS group between 1 and 2 years and 1 and 3 years. The lumen area remained unchanged in the BVS group between 1 and 4 years but decreased by 34% in the EES group. Abbreviations as in Figure 1.

reported here (8), suggesting that untreated atherosclerosis amplified late lumen loss and stenosis progression in our study. These data are consistent with preclinical observations in normal swine (15) and with clinical observations described in the ABSORB II randomized trial, in which BVS showed frequent dynamic vessel remodeling with larger increase in mean lumen and vessel area compared to the EES at 3 years (16). With regard to other histological findings, the notable disparity between EES and BVS in inflammation/macrophages at 4 years presumably results from the continued presence of metallic struts with EES compared to complete resorption and tissue replacement for BVS. Otsuka et al. (8) reported mild to moderate inflammation in BVS through 42 months in the healthy swine model, and the observed inflammation progressively decreased, with largely restored morphological appearance of BVS-implanted arteries after 18 months, which is the same period during which the most rapid mass loss occurred. However, although EES has demonstrated preclinical and clinical safety with low inflammation to 4 years and beyond, the sustained inflammation observed in the treated arterial segments at years 3 and 4 is likely a function of the inherent highly inflammatory state of the arteries in the unmitigated atherosclerotic model used in our study.

This study has confirmed that complete scaffold resorption occurs between years 3 and 4 in the presence of atherosclerosis. At 4 years, the struts are no longer visible on OCT, and histological evaluation confirmed the full integration of the device described as connective tissue replacing the pre-existing polymeric struts. These findings indicate that the scaffold bioresorption timeline defined in normal animals (8,17) is not significantly altered by atherosclerosis. Unlike in healthy animals, severe atherosclerosis was present in all vessels evaluated, and significant disease progression was evident up to 4 years. The severity of the disease is not unexpected in this model and is likely attributed to the 4-year chronic exposure to supra-physiological levels of cholesterol in the absence of any cholesterol-lowering therapy. Indeed, the high cholesterol levels (>350 mg/dl) likely exacerbated the progression of atherosclerosis in this study. This was readily evidenced by the severity of atherosclerosis observed in the proximal and distal host (nonimplanted) regions.

The speculation that a more prolonged polymer resorption process may have taken place in patients with complex and biologically active atherosclerosis originated from the clinical observations that uncovered intraluminal dismantling has been associated with the late biomechanical failure of the device (18).

FIGURE 6 **Histologic Appearance of BVS and EES Over Time**

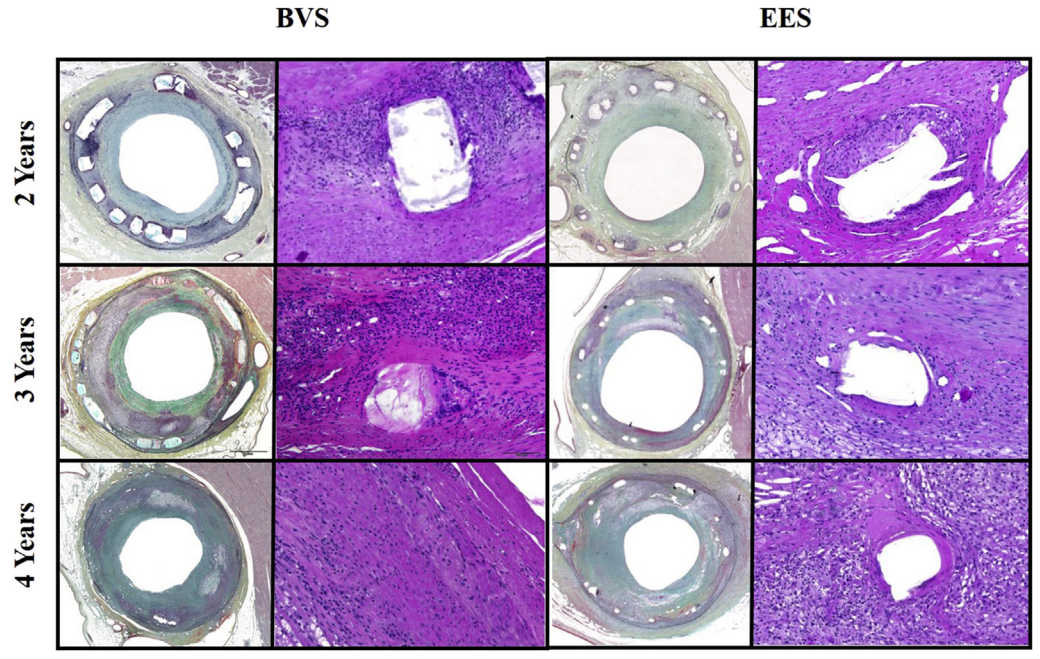

Representative low (original magnification: ×2) and high (original magnification: ×20) power images of BVS- and EES-implanted vessels at 2, 3, and 4 years. Sections shown are stained by **(left)** MP (original magnification: ×2), and **(right)** HE (original magnification: ×20). Abbreviations as in Figure 1.

However, late discontinuities are part of the normal late phase of the scaffold dismantling process when adequately covered with tissue. In the present study, there were no malapposed struts observed at baseline in this study; atypical alignment or strut stacking was seen infrequently in BVS sections at 2 and 3 years and may represent localized structural discontinuities. All the struts were completely embedded and incorporated with neointimal growth; hence, no adverse events occurred during the follow-up period. Therefore, in view of our study demonstrating a similar polymer resorption timeline in the presence of atherosclerosis, it is plausible that the intraluminal dismantling observed clinically is not caused by delayed polymer resorption but, rather, by long-term adverse biomechanical consequences of problematic deployment.

Finally, the responses to BVS and EES in this study were comparable, with similar neointimal character and inflammation and injury scores. Additionally, evidence of neoatherosclerosis (necrotic core, foam cells, cholesterol clefts and calcification) was observed over time to an equivalent degree in both devices. Human autopsy studies suggest that neoatherosclerosis in drug-eluting stent shows unstable characteristics by 2 years after implantation (19), and neoatherosclerosis development may relate to dysfunctional vessel healing, persistent inflammation, platelet activation, and adverse immunologic responses (20). In our study, neointimal inflammation was moderate to severe in both devices tested, and neoatherosclerosis was evident by the second year after device implantation. These data are important because they show that BVS, also being a drug-eluting device, is not immune to neoatherosclerosis formation. The INVEST (INdependent OCT Registry on VEry Late Bioresorbable Scaffold Thrombosis) registry (21), which represents the largest cohort and first international multicenter consortium to investigate the mechanisms underlying very late scaffold thrombosis, has found that neoatherosclerosis was observed as a mechanism underlying late scaffold thrombosis in 18.4% of lesions at 26.9 ± 11.3 months after BVS implantation.

Several limitations were present in the current study. First, EES was implanted in larger vessels due to stent size availability, but this was offset by normalizing the results to the stent/scaffold size, and efforts were made to keep the arterial injury consistent, irrespective of anatomic location and device type by rigorous control of stent-to-artery ratio. Second, the sample size is modest in

FIGURE 7 Representative Histological Images of Neoatherosclerosis

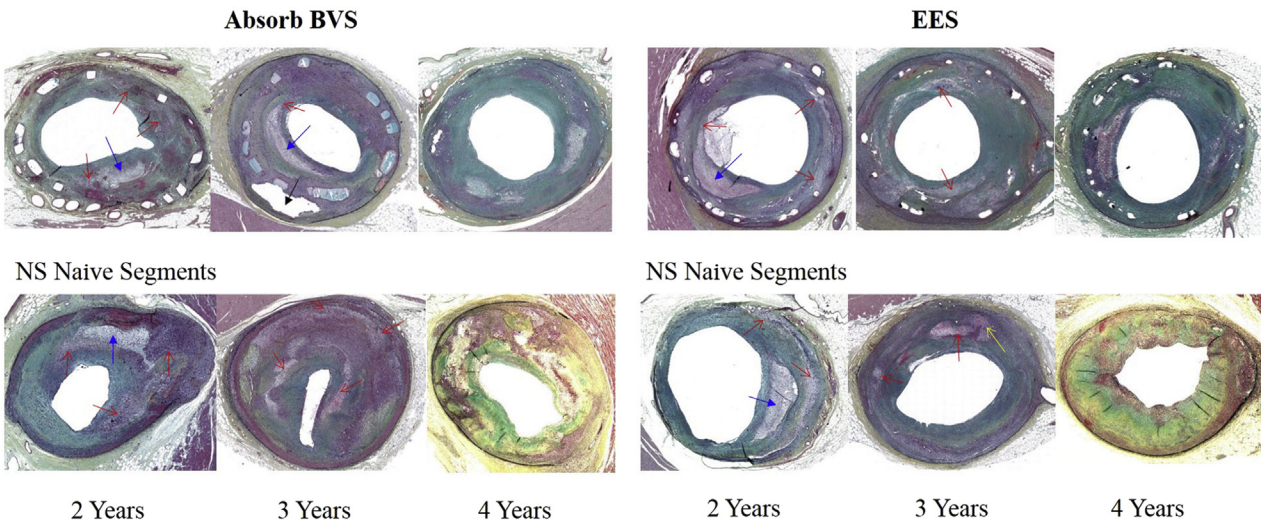

Representative histological images of neoatherosclerosis in BVS- and EES-implanted sections and atherosclerosis in proximal/distal reference segments (NS) at 2 to 4 years. Atherosclerosis with necrotic core **(blue arrow)**, foamy macrophages **(red arrows)**, cholesterol clefts **(yellow arrow)**, and calcification **(black arrow)** in the device implanted and proximal/distal naïve segments. Sections shown are stained by MP (original magnification: ×2).

comparison to previous studies in normal animals, the study was not longitudinal, and the imaging observations could not be serial; still, valuable insights were rendered. Finally, our diseased model still differs from atherosclerosis seen in human coronary arteries, and the absence of cholesterol-lowering therapy routinely expected in patients treated for obstructive coronary disease presumably augments this difference. However, although the resulting lesions may be biologically different, we have shown that the diseased vascular background used in this study may unveil differences in vascular healing otherwise not shown by healthy animal models.

FIGURE 8 Summary of Key Semiquantitative Histology Parameters

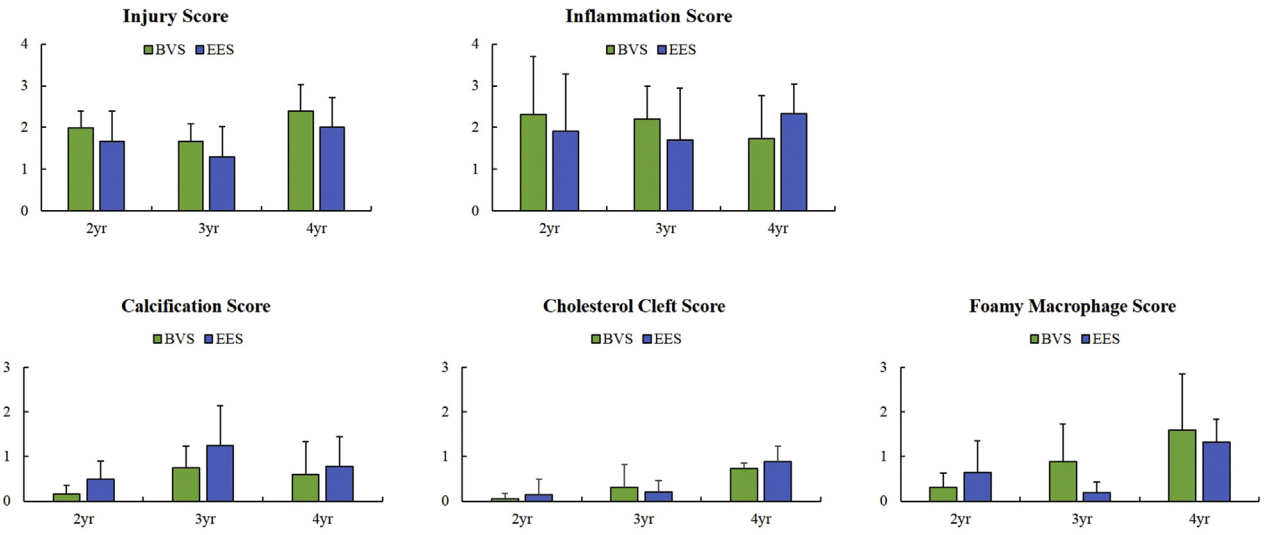

Histological analysis showed comparable vascular healing responses and evidence of neoatherosclerosis between BVS and EES from 2 to 4 years. Abbreviations as in Figure 1.

CONCLUSIONS

In the presence of untreated hyperlipidemia and atherosclerosis, by using multimodality imaging and histology, BVS demonstrates comparable long-term vascular healing and anti-restenosis efficacy compared with EES, with lower late lumen loss at 4 years attributable to favorable remodeling not attainable in the EES-caged segments. In addition, the integration process is complete at 4 years based on OCT and histological findings, indicating that the scaffold bioresorption/integration timeline defined in normal animals is not significantly altered by atherosclerotic disease.

ADDRESS FOR CORRESPONDENCE: Dr. Juan F. Granada, CRF Skirball Center for Innovation, Cardiovascular Research Foundation, 8 Corporate Drive, Orangeburg, New York 10962. E-mail: jgranada@crf.org.

PERSPECTIVES

COMPETENCY IN MEDICAL KNOWLEDGE: The biological effect of BVS on atherosclerotic plaque progression and its effect on neointimal formation and composition have not been well studied. This long-term (up to 4 years) study using multimodality imaging and histology shows that the implantation of BVS in an untreated animal model of atherosclerosis resulted in expansive vascular remodeling and slower late lumen loss compared to EES but a similar extent of neoatherosclerosis.

TRANSLATIONAL OUTLOOK: Imaging and histology demonstrate that BVS degradation follows the same progression in the presence of atherosclerosis as it does in normal arteries; however, BVS is not immune to the development of neoatherosclerosis.

REFERENCES

1. Palmerini T, Benedetto U, Biondi-Zoccai G, et al. Long-term safety of drug-eluting and bare-metal stents: evidence from a comprehensive network meta-analysis. J Am Coll Cardiol 2015;65:2496–07.

2. Mahmoud AN, Shah NH, Elgendy IY, et al. Safety and efficacy of second-generation drug-eluting stents compared with bare-metal stents: an updated meta-analysis and regression of 9 randomized clinical trials. Clin Cardiol 2018;41:151–8.

3. Niccoli G, Sgueglia GA, Montone RA, Roberto M, Banning AP, Crea F. Evolving management of patients treated by drug-eluting stent: prevention of late events. Cardiovasc Revasc Med 2014;15:100–8.

4. Onuma Y, Muramatsu T, Kharlamov A, Serruys PW. Freeing the vessel from metallic cage: what can we achieve with bioresorbable vascular scaffolds? Cardiovasc Interv Ther 2012;27:141–54.

5. Stone GW, Gao R, Kimura T, et al. 1-year outcomes with the Absorb bioresorbable scaffold in patients with coronary artery disease: a patient-level, pooled meta-analysis. Lancet 2016;387:1277–89.

6. Ali ZA, Serruys PW, Kimura T, et al. 2-year outcomes with the absorb bioresorbable scaffold for treatment of coronary artery disease: a systematic review and meta-analysis of seven randomised trials with an individual patient data substudy. Lancet 2017;390:760–72.

7. Ali ZA, Gao R, Kimura T, et al. Three-year outcomes with the absorb bioresorbable scaffold: individual-patient-data meta-analysis from the ABSORB randomized trials. Circulation 2018;30:464–79.

8. Otsuka F, Pacheco E, Perkins LE, et al. Long-term safety of an everolimus-eluting bioresorbable vascular scaffold and the cobalt-chromium Xience V stent in a porcine coronary artery model. Circ Cardiovasc Interv 2014;7:330–42.

9. Tellez A, Seifert PS, Donskoy E, et al. Experimental evaluation of efficacy and healing response of everolimus-eluting stents in the familial hypercholesterolemic swine model: a comparative study of bioabsorbable versus durable polymer stent platforms. Coron Artery Dis 2014;25:198–207.

10. Pedersen SF, Thrysøe SA, Paaske WP, et al. CMR assessment of endothelial damage and angiogenesis in porcine coronary arteries using gadofosveset. J Cardiovasc Magn Reson 2011;13:10.

11. Vahl TP, Gasior P, Gongora CA, et al. Four-year polymer biocompatibility and vascular healing profile of a novel ultrahigh molecular weight amorphous PLLA bioresorbable vascular scaffold: an OCT study in healthy porcine coronary arteries. EuroIntervention 2016;12:1510–8.

12. Onuma Y, Serruys PW, Perkins LE, et al. Intracoronary optical coherence tomography and histology at 1 month and 2, 3, and 4 years after implantation of everolimus-eluting bioresorbable vascular scaffolds in a porcine coronary artery model: an attempt to decipher the human optical coherence tomography images in the ABSORB trial. Circulation 2010;122:2288–300.

13. Otsuka F, Byrne RA, Yahagi K, et al. Neoatherosclerosis: overview of histopathologic findings and implications for intravascular imaging assessment. Eur Heart J 2015;36:2147–59.

14. Zhao HQ, Nikanorov A, Virmani R, Schwartz LB. Inhibition of experimental neointimal hyperplasia and neoatherosclerosis by local, stent-mediated delivery of everolimus. J Vasc Surg 2012;56:1680–8.

15. Lane JP, Perkins LEL, Sheehy AJ, et al. Lumen gain and restoration of pulsatility after implantation of a bioresorbable vascular scaffold in porcine coronary arteries. J Am Coll Cardiol Intv 2014;7:688–95.

16. Serruys PW, Katagiri Y, Sotomi Y, et al. Arterial remodeling after bioresorbable scaffolds and metallic stents. J Am Coll Cardiol 2017;70:60–74.

17. Campos CM, Ishibashi Y, Eggermont J, et al. Echogenicity as a surrogate for bioresorbable everolimus-eluting scaffold degradation: analysis at 1-, 3-, 6-, 12- 18, 24-, 30-, 36- and 42-month follow-up in a porcine model. Int J Cardiovasc Imaging 2015;31:471–82.

18. Stone GW, Granada JF. Very late thrombosis after bioresorbable scaffolds. Cause for concern? J Am Coll Cardiol 2015;66:1915–7.

19. Park SJ, Kang SJ, Virmani R, Nakano M, Ueda Y. In-stent neoatherosclerosis: a final common pathway of late stent failure. J Am Coll Cardiol 2012;59:2051–7.

20. Borovac JA, D'Amario D, Vergallo R, et al. Neoatherosclerosis after drug-eluting stent implantation: a novel clinical and therapeutic challenge. Eur Heart J Cardiovasc Pharmacother 2019;5:105–16.

21. Yamaji K, Ueki Y, Souteyrand G, et al. Mechanisms of very late bioresorbable scaffold thrombosis: the INVEST registry. J Am Coll Cardiol 2017;70:2330–44.

KEY WORDS bioresorbable vascular scaffolds, familial hypercholesterolemic swine, metallic drug-eluting stents, neoatherosclerosis